



Cite this: *Soft Matter*, 2025, 21, 2723

Received 30th January 2025,  
Accepted 17th March 2025

DOI: 10.1039/d5sm00099h

[rsc.li/soft-matter-journal](http://rsc.li/soft-matter-journal)

## On the existence of prewetting in supercritical fluid mixtures

Jan Forsman<sup>ib</sup>\*<sup>a</sup> and Clifford E. Woodward<sup>b</sup>

We demonstrate the existence of a first-order prewetting transition of a supercritical model polymer solution adjacent to an attractive surface. The model fluid we use mimics (qualitatively) an aqueous polyethylene oxide solution and, like the actual solution, displays a closed loop 2-phase region with an upper and lower critical solution temperature. The model fluid is shown to undergo a prewetting transition at an adjacent attractive surface. For sufficiently strong surface affinities, the prewetting transition may occur even at temperatures below the lower critical solution temperature (supercriticality). This phenomenon follows from non-local thermodynamics when the length-scale of the relevant fluid structures of surface films are commensurate or smaller than the range of intermolecular interactions.

### 1. Introduction

Many binary fluid mixtures or solutions display a demixing phase diagram with both an upper and a lower critical solution temperature (U/LCST), which bracket the 2-phase region. Above the UCST and below the LCST, in what we will refer to as the supercritical regions, the mixture exists as a single phase. In this article, we will be primarily concerned with the supercritical region below the LCST.

#### 1.1. Background

The presence of an LCST is not common in mixtures of simple fluids (examples include nicotine-water and triethylamine-water), but in polymer solutions it is more the rule rather than the exception.<sup>1–7</sup> One example is an aqueous solution of poly(ethylene oxide) (PEO) which has an LCST that approaches 100 °C at high molecular weights.<sup>8</sup> Using classical polymer density functional theory (cDFT), we have generalised a successful theoretical model for such solutions,<sup>4</sup> that can be used to model these solutions in heterogeneous environments.<sup>9–11</sup> In this model, monomers are assumed to be in either of two classes of states, labelled A and B, where B is more solvophobic than A. Thus A states become preferred as the temperature is lowered, which promotes complete dissolution. On the other hand, the degeneracy of the B class exceeds that of A, which means the relative probability of B (solvophobic) monomers increases with temperature. This creates the possibility of demixing with increasing temperature, leading to an LCST. At a high enough temperature, the mixing entropy dominates interactions, giving rise to an UCST. We do not resort

to temperature-dependent interactions per se, but instead make explicit the intrinsic enthalpic and entropic contributions of A and B species within an aqueous environment.

Consider a bulk mixture which is able to diffuse freely into and out of a pore. If the pore surfaces interact directly with the confined fluid, they may cause a phase change relative to the bulk fluid, so-called capillary induced phase separation (CIPS).<sup>12</sup> If we make the assumption that the fluid–fluid interactions are short-ranged compared to the size of the pore then the pore will only contribute surface terms to the free energy and CIPS can only occur if the bulk fluid is not supercritical. In pores which are narrow compared to the range of fluid–fluid interactions, there may be a significant shift along the temperature axis of the 2-phase region of the confined fluid. This is because surfaces will truncate intermolecular interactions between fluid particles.<sup>12–15</sup> As these interactions are generally attractive at long range (at least for non-ionic fluids) this causes a decrease in the cohesive forces within the fluid. To illustrate, consider a single-component fluid displaying a critical temperature. Reduction in the cohesive forces, due to truncation, will mean the confined fluid behaves similarly to that of the bulk fluid, but at a higher temperature. Thus the overall phase diagram of the confined fluid is shifted to lower temperatures, compared to that of the bulk.<sup>14</sup> Such a situation is still consistent with the requirement above, *i.e.*, CIPS can only occur if the temperature of the bulk fluid is below the critical temperature. However, the scenario is more complex for mixtures that display an LCST in the bulk. In previous work, we have shown that confining the mixture in a pore reduces the LCST.<sup>9–11</sup> Thus, in this case, the confined fluid may undergo CIPS, even though the bulk solution is supra-critical. Such transitions may occur also with inert surfaces.<sup>11</sup>

Some fluids may undergo first-order phase transitions at a single surface *via* so-called “thin-thick” (prewetting) transitions. These are surface transitions, as the prewetting phases involve

<sup>a</sup> Computational Chemistry, Lund University, P.O.Box 124, S-221 00 Lund, Sweden.  
E-mail: [jan.forsmancompchem.lu.se](mailto:jan.forsmancompchem.lu.se)

<sup>b</sup> School of Physical, Environmental and Mathematical Sciences University College, University of New South Wales, ADFA, Canberra, ACT 2600, Australia



structural changes of the fluid that are intrinsically confined to narrow films adjacent to the adsorbing surface. Thus, the truncation of fluid–fluid interactions discussed above will plausibly also affect prewetting transitions. In particular, according to the discussion above, one expects that the UCST of the prewetting transition is lower than that of the bulk phase transition. On the other hand, the role of these mechanisms in the vicinity of an LCST has hitherto not attracted significant attention in the literature, as far as we are aware.

### 1.2. Qualitative considerations

Consider a bulk 2-component solution, at some fixed pressure and temperature,  $T$ . This mixture possesses a demixing regime wherein the fluid separates into a concentrated,  $C$ , and dilute,  $D$ , phase with respect to one of the components (the “solute” species). For the moment, we will assume that this solution displays only a UCST. The prewetting behaviour of such systems are well established,<sup>16–21</sup> but it is useful to recapitulate the main concepts. Suppose such a solution in its undersaturated  $D$  phase,  $T < \text{UCST}$ , is adjacent to a single surface,  $W$ , which is attractive to the solute species. A positive adsorption of solute at the surface gives rise to what we will label a “thin” surface film of excess solute. The surface tension at the surface–fluid interface is denoted as,  $\gamma_{\text{WD}}$ . Making the bulk fluid more concentrated will cause an increase in the excess solute adsorption. Above the so-called wetting temperature,  $T_{\text{W}}$ , this increasing adsorption will grow by way of a thickening film, with width  $L$ . The fluid in this film will have a character similar to the metastable  $C$  phase and the surface–fluid interfacial tension will approach  $\gamma_{\text{WC}}$ . This occurs because  $\gamma_{\text{WC}} < \gamma_{\text{WD}}$  and the free energy is lowered accordingly. However, the film also establishes a  $C$ – $D$  interface with the bulk and the ensuing positive surface tension contribution,  $\gamma_{\text{CD}}$ , will act to counter the free energy lowering at the adsorbing surface. At saturation (*i.e.*, on the bulk coexistence curve), the free energy penalty for growing a film ( $L \rightarrow \infty$ ) approaches  $\Delta\gamma$  ( $= \gamma_{\text{WC}} + \gamma_{\text{CD}} - \gamma_{\text{WD}}$ ), from above, where the surface tensions are defined with respect to the coexisting  $C$  and  $D$  phases. For  $T > T_{\text{W}}$ ,  $\gamma_{\text{CD}}$  is sufficiently small so that,  $\Delta\gamma < 0$ , and the film grows to infinity spontaneously. This gives rise to a divergence in the excess adsorption of solute and complete wetting. For  $T < T_{\text{W}}$ ,  $\gamma_{\text{CD}}$  is large enough that  $\Delta\gamma > 0$ : the thin film persists and no wetting layer forms (partial wetting).

As stated earlier, in some cases, the film thickness may grow discontinuously, undergoing a first-order, so-called “thin-thick” (or prewetting) transition, at some undersaturated value of  $D$ . The locus of concentrations (*versus*  $T$ ) where this transition occurs, is called the prewetting line. This line intercepts the bulk coexistence line at,  $T_{\text{W}}$ , and terminates at some upper, prewetting critical temperature,  $\text{UCST}_{\text{pw}} < \text{UCST}$ . This last inequality occurs due to the truncation mechanism described earlier, which applies here because of the finite width of the fluid films that coexist on the prewetting line. The free energy (per unit area) cost for film formation at  $T > T_{\text{W}}$  in an undersaturated bulk solution can be written as  $\Delta\gamma + \Delta F_{\text{CD}}(L)$ . Here,  $\Delta F_{\text{CD}}(L) > 0$  is essentially the intrinsic free energy of the thick fluid film, without the contributions from the wall–fluid and fluid–fluid surface terms. If  $\Delta f_{\text{CD}}$  denotes the difference in free energy per unit volume of

the metastable bulk  $C$  phase relative to the stable bulk  $D$  phase (at the same temperature and pressure), then we have  $\Delta F_{\text{CD}}(L) \approx \Delta f_{\text{CD}}L$  for large enough  $L$ . The prewetting transition occurs because the system admits two stable film phases on the prewetting line. For  $T = T_{\text{W}}$  we have  $\Delta F_{\text{CD}}(L) = \Delta\gamma = 0$ .

In particular, according to the discussion above, one expects that the UCST of the prewetting transition is lower than that of the bulk phase transition. We should note that this phenomenon is not universal, *e.g.*, type I superconductors (SC) can display a prewetting like transition above the critical temperature. This is due to the enhancement of the SC transition at surfaces, leading to nucleation of finite width layers that merge with the prewetting line.<sup>22</sup>

So what happens for a mixture which also possesses an LCST as well? As argued above for the case of a UCST only,  $T_{\text{W}}$ , primarily arises due to the increase in  $\gamma_{\text{CD}}$  as the temperature decreases. This is correlated with the increasing compositional differences between coexisting bulk  $C$  and  $D$  phases, as the temperature decreases. When an LCST is present, the 2-phase region becomes a closed loop, which causes  $\gamma_{\text{CD}}$  to decrease again as  $T$  decreases toward the LCST. This gives rise to the possibility that both an upper and lower wetting temperature exist, giving rise to two prewetting lines, respectively terminating above at  $\text{UCST}_{\text{pw}}$  and below at  $\text{LCST}_{\text{pw}}$  (“case (i)”). Within the case (i) scenario, we also include systems which possess either an upper or lower prewetting line alone. On the other hand, it is possible that one or both prewetting lines will detach from the coexistence line. This would result in at least one prewetting line of finite length, as shown in Fig. 1 (“case (ii)”), and complete wetting as one approaches the bulk coexistence line.

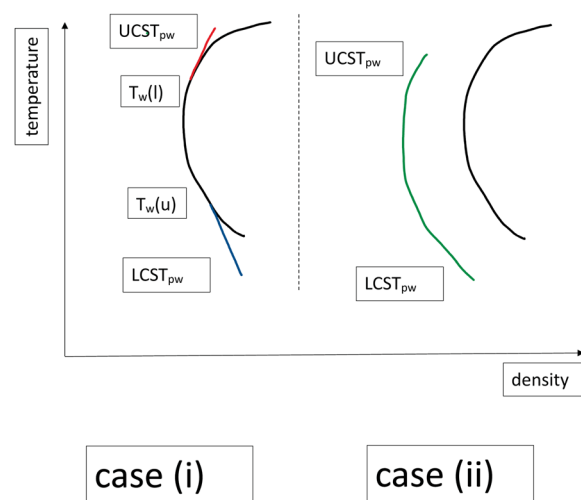


Fig. 1 An illustration of two possible scenarios. In “case (i)”, there is a lower prewetting line, that terminates tangentially on the bulk coexistence line, at an upper wetting temperature,  $T_{\text{W}}(u)$ . This lower prewetting line may extend to lower temperatures, ending at a lower ( $\text{LCST}_{\text{pw}}$ ) critical prewetting temperature. In addition, there is an upper prewetting line with a lower wetting temperature,  $T_{\text{W}}(l)$ , terminating at an upper critical point, ( $\text{UCST}_{\text{pw}}$ ). There is also a possibility that just one of these prewetting lines is present. In “case (ii)”, the prewetting lines may be detached from the bulk coexistence curve. Here we depict a detached prewetting line bound by upper and lower ( $\text{LCST}_{\text{pw}}$ ) critical prewetting temperatures. The former is always below the bulk UCST, but  $\text{LCST}_{\text{pw}}$  may be located below the bulk LCST.



Furthermore, due to truncation of intermolecular forces in the finite films of prewetting phases, as described above, we also anticipate a possibility that  $LCST_{pw} < LCST$ , see Fig. 1. This suggests the fascinating option of thin-thick transitions under supraccritical conditions (supraccritical prewetting). That is, at some temperatures, lower than LCST, prewetting transitions occur but don't signal the onset of film growth on the surface as the bulk solution concentration increases. Thus the excess solute adsorption always remains finite at all bulk concentrations. In this sense, the term "prewetting transition" becomes something of a misnomer. That is, while the system can undergo a thin-thick transition it does not lead to complete wetting as the composition increases. This underlines the fact that the prewetting transition is essentially a surface transition and is not intrinsically dependent on complete wetting in any fundamental sense.

## 2. Model and theory

Following this qualitative discussion, we will now turn to quantitative predictions. In particular, we will use the aqueous PEO solution model described earlier. This will require some model details, and definitions. We let  $N(\mathbf{R})$  denote the density distribution of monodisperse PEO polymers with  $r$  monomers. Here,  $\mathbf{R} = \mathbf{r}_1, \mathbf{r}_2, \dots, \mathbf{r}_r$ , where  $\mathbf{r}_i$  is the coordinate of monomer  $i$ . The polymers are assumed linear with monomers joined by freely rotating bonds, described by a potential  $V_b$ . This potential is chosen to ensure a constant bond length  $b$ , i.e.  $e^{-\beta V_b(\mathbf{R})} \propto \prod \delta(|\mathbf{r}_{i+1} - \mathbf{r}_i| - b)$ , where  $\delta(x)$  is the Dirac delta function, and  $\beta = 1/(kT)$  is the inverse thermal energy. We will assume that the total mixture (polymer and solvent) is incompressible. This is ensured by constraining the total density of monomers + solvent particles to a fixed value,  $n_t$ , i.e.  $n_t = n(\mathbf{r}) + n_s(\mathbf{r})$ , where  $n(\mathbf{r})$  and  $n_s(\mathbf{r})$  are the monomer and solvent densities at position  $\mathbf{r}$ . Specifically, we have set  $n_t \sigma^3 = 1$ , where  $\sigma$  is the Lennard-Jones length parameter, common to all species, as defined below. According to our description above, we introduce the monomer state probabilities  $P_A$  and  $P_B$ , and defining state densities  $n_A(\mathbf{r}) \equiv n(\mathbf{r})P_A(\mathbf{r})$  and  $n_B(\mathbf{r}) \equiv n(\mathbf{r})(1 - P_A(\mathbf{r}))$ , we write the fluid free energy density functional,  $F$ , as:

$$\begin{aligned} \beta F = & \int N(\mathbf{R})(\ln[N(\mathbf{R})] - 1) d\mathbf{R} + \beta \int N(\mathbf{R}) V_b(\mathbf{R}) d\mathbf{R} \\ & + \int (n_S(\mathbf{r}) \ln[n_S(\mathbf{r})] + n(\mathbf{r})) d\mathbf{r} \\ & + \frac{\beta}{2} \sum_{\alpha, \beta} \iint n_\alpha(\mathbf{r}) n_\beta(\mathbf{r}') \phi_{\alpha\beta}^{(a)}(|\mathbf{r} - \mathbf{r}'|) d\mathbf{r}' d\mathbf{r} \\ & + \int n_A(\mathbf{r}) \ln \left[ \frac{P_A(\mathbf{r})}{g_A} \right] d\mathbf{r} \\ & + \int n_B(\mathbf{r}) \ln \left[ \frac{1 - P_A(\mathbf{r})}{g_B} \right] d\mathbf{r} \\ & + \beta \sum_{\alpha, \beta} \int n_\alpha(\mathbf{r}) V_{\text{ex}}^z(\mathbf{r}) d\mathbf{r} \end{aligned} \quad (1)$$

where we have included an external (surface) potential,  $V_{\text{ex}}^z(\mathbf{r})$ , that acts on the  $\alpha$  particles, with  $\alpha = A, B$  or  $S$ . Recall that these denote

solvophilic monomers (A), solvophobic monomers (B), and solvent particles (S). The degeneracies of monomer classes A and B are denoted  $g_A$  and  $g_B$ .

All particles (monomers and solvent) particles have a hard core with diameter,  $\sigma$ , and interact with each other *via* a Lennard-Jones (L-J) potential,  $\phi_{\alpha\beta}^{(a)}(r)$ :

$$\phi_{\alpha\beta}^{(a)}(r) = 4\epsilon_{\alpha\beta} \left( \left( \frac{\sigma}{r} \right)^{12} - \left( \frac{\sigma}{r} \right)^6 \right), \quad r > \sigma \quad (2)$$

Defining a reference energy parameter,  $\epsilon_{\text{ref}}$ , we obtain reduced parameters  $\epsilon_{\alpha, \beta}^* \equiv \epsilon_{\alpha, \beta} / \epsilon_{\text{ref}}$ , as well as a reduced temperature  $T^* = kT / \epsilon_{\text{ref}}$ . We will use the same energy parameters as in our previous studies.<sup>9-11</sup> In that model, the parameters are shifted so that all long-range AA, AS and SS interactions vanish, i.e.,  $\epsilon_{AA}^* = \epsilon_{SS}^* = \epsilon_{AS}^* = 0$ , while  $\epsilon_{BB}^* = \epsilon_{SB}^* = -0.7$ , and  $\epsilon_{AB}^* = \sqrt{0.3} - 1 \approx -0.45$ . We have previously shown that for  $g_A/g_B = 13$ , one obtains a bulk fluid with both a UCST and an LCST, for long enough chains.<sup>10</sup> Note that this means that we are employing spherically symmetric interactions, which obviously differ from (say) the PEO/water system. Directional interactions may often be relevant but in this generic work we show that such properties are not required to produce the behaviours we seek to elucidate.

The potential function,  $V_{\text{ex}}^z(\mathbf{r})$ , defines the nature of the surface, which is modelled as a hard flat wall parallel to the  $(x, y)$  plane (with  $z$  normal). We set:

$$V_{\text{ex}}^z(z) = \begin{cases} \infty, & z < 0 \\ W_z[w(z) - w(z_c)], & 0 < z < z_c \\ 0, & z > z_c \end{cases} \quad (3)$$

where  $w(z) = (1 - e^{-z/\sigma})^2 - 1$ , and  $z_c = 10\sigma$ . In this case, we chose  $W_A = W_S = 0$ , which allows us to regulate the surface properties by a single parameter,  $W_B^* \equiv W_B / \epsilon_{\text{ref}}$ , that determines the affinity to B. The adsorption potential is illustrated in Fig. 2, under conditions that are typical to this work. We note that, although the wall potential is formally limited by  $z_c$ , it actually decays quite fast, and becomes almost insignificant beyond  $3\sigma$  or so. We emphasise that in the present generic work the

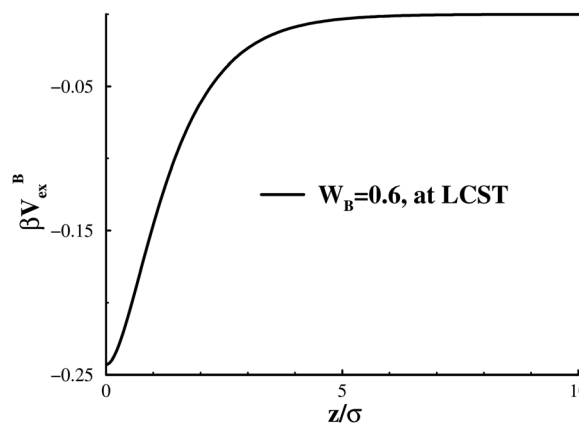


Fig. 2 An illustration of the surface adsorption potential, normalised by thermal energy, with  $W_B = 0.6$ , at the LCST.



specific functional form of this short-ranged adsorption potential is qualitatively irrelevant, and we could instead have chosen (say) a square well potential.

The grand potential is defined as,  $\Omega = F/A - \int \mu_p n(z) dz$ , where  $\mu_p$  is the polymer chemical potential and  $A$  is the surface area of the walls, which we assume is infinite. The functional,  $\Omega$ , is then minimised with respect to both  $n(z)$  and  $P_x(z)$  to obtain the equilibrium density profiles of the different monomer species and the incompressibility constraint allows us to infer the solvent density profile. The net reduced monomer adsorption,  $\Gamma^*$ , is obtained as  $\Gamma^* = \int_0^\infty (n(z) - n_b) \sigma^3 dz$ , where  $n_b$  is the bulk monomer density. Integrals are solved on a grid (along  $z$ ), up to some large distance ( $H = 50\sigma$  or  $100\sigma$ , depending on conditions), beyond which bulk conditions are assumed. Test calculations were performed to verify convergence, *i.e.* that we have used a fine enough grid, and a large enough value of  $H$ .

### 3. Results

Using this type of surface model, we have established that a prewetting transition can occur in a 300-mer polymer solution. In Fig. 3 we show the prewetting phase diagram,  $\Gamma^*$  vs.  $T$ , for surface attractions ( $W_B$ ) that are strong enough to result in “case (ii)” behaviour. The temperature is scaled with respect to the bulk LCST. The prewetting transition describes a closed loop over the range,  $UCST_{pw}$  to  $LCST_{pw}$ , which indicates that the prewetting line is completely detached from the bulk 2-phase line and there are no wetting temperatures. Furthermore, we see that both prewetting critical temperatures are below their bulk counterparts. This confirms that prewetting transitions can occur in supercritical regions of the bulk fluid.

In Fig. 4 we show the prewetting line together with the dilute part of the bulk coexistence region, for a range of surface

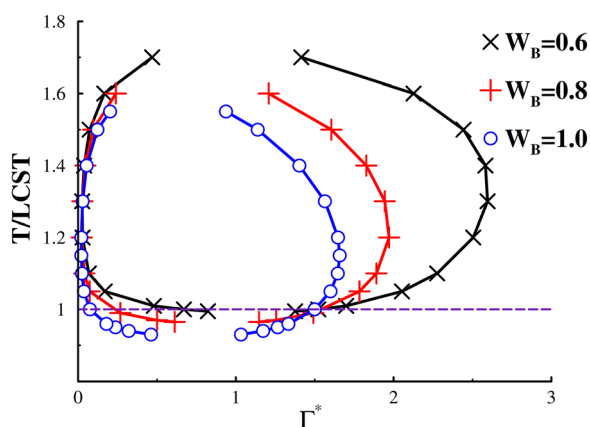


**Fig. 3** Thin-thick coexistence curves, for a 300-mer polymer solution that displays an LCST. Crosses, plus signs, and circles denote various strengths of a short-ranged B-specific adsorption potential (see eqn (3)), with circles denoting the strongest attraction. Note that in the latter case, the lower critical surface temperature is about 8% below the LCST. For PEO/water this would correspond to about 30 °C. All these systems are of “case (ii)” type, *i.e.* there is no upper wetting temperature. Instead, the thin and thick phases merge at some upper critical temperature.

potential strengths. Here, we also include results with quite weak adsorption, whereby “case (i)” scenarios emerge (dashed lines), *i.e.* prewetting lines that terminate at bulk coexistence conditions, thereby defining an upper wetting temperature. In those cases, the prewetting line does not proceed below the LCST. It is not immediately obvious that one could not find “case (i)” systems for which the lower critical prewetting temperature is lower than the LCST. Nevertheless, we were unable to establish such a scenario for the systems that we have investigated in this work. We also note that it is at least possible that thin-thick transitions may take place at an inert surface, without preferential attraction to any fluid species. This is because of the unequal mutual interactions between species, *i.e.*, the system can minimise the wall–fluid interfacial tension by preferential adsorption of species with weaker interactions. For example, such a mechanism gives rise to CIPS in narrow inert pores.<sup>9,11</sup> We have so far only established thin-thick coexistence for surfaces that are somewhat more attractive to the solvophobic B monomers for the current model. On the other hand, the surface attractions required are short-ranged, and quite weak, so we do not rule out that one might observe prewetting transitions for non-adsorbing surfaces with other interaction models. We also note, in Fig. 4, that the “case (i)” systems lack an upper prewetting line, for the systems that we have investigated here.

In Fig. 5, we give an example of density profiles for coexisting thin and thick phases; in this case at a temperature corresponding to the bulk LCST. These merge together at  $LCST_{pw}$ . The two phases are quite similar, since we are relatively close to the lower prewetting temperature,  $LCST_{pw}$ . Nevertheless, it is quite clear that two phases remain discernable, despite critical conditions in the bulk.

In Fig. 6 we illustrate a fundamental difference between “ordinary” prewetting (above LCST) and supercritical prewetting (below LCST). In the former case, the net adsorption diverges as we increase the bulk phase concentration towards the bulk coexistence line. For supercritical adsorption, the thickness remains finite for all bulk concentrations and, indeed, the net adsorption decreases at some point, as the

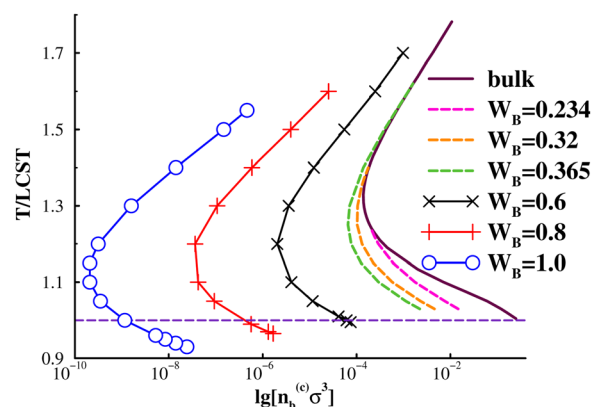


**Fig. 4** Prewetting lines for 300-mer polymer solution that displays an LCST.  $n_b^{(c)}$  denotes the bulk density at thin-thick coexistence. Upper prewetting temperatures,  $T_w(u)$  are obtained for three adsorption strengths:  $T_w(u, 0.234)/LCST \approx 1.24$ ,  $T_w(u, 0.32)/LCST \approx 1.41$ ,  $T_w(u, 0.234)/LCST \approx 1.62$ .



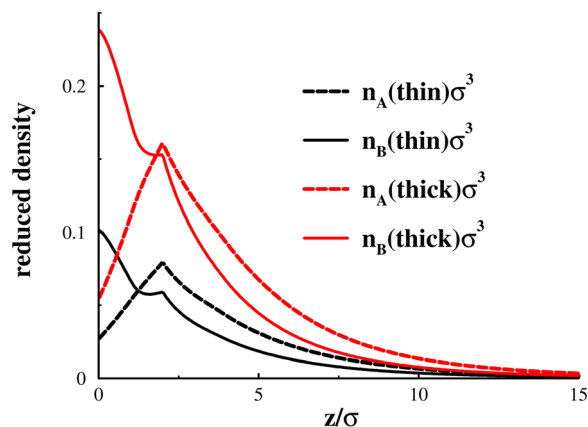


Fig. 5 Density profiles, for coexisting thin (black) and thick (red) phases, for a 300-mer solution, at the bulk LCST, with  $W_B^* = 0.6$ . Separate profiles for A (dashed) and B (solid) type are displayed.

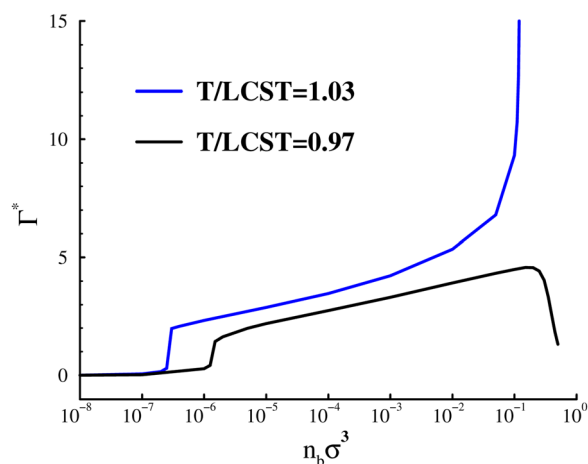


Fig. 6 The dependence of net adsorption on bulk concentration above and below the LCST. The “jump” at low concentrations signifies the first-order prewetting transition. The results are for a 300-mer solution, with  $W_B^* = 0.8$ .

bulk concentration increases, due to polymer depletion and the lower energy per monomer in the bulk.

The transitions will also depend upon the length of the polymer chains. In Fig. 7, we compare our results for 300-mer mixtures, with a corresponding phase diagram for a 100-mer mixture. Adsorption of polymers is a cooperative process, and with shorter polymers a stronger surface affinity of B-type monomers is required, in order to push the lower critical surface temperature below the bulk LCST. In this case, we have set  $W_B^* = 1.5$  for the 100-mers, which leads to a similar  $T/LCST$  ratio at the lower surface critical temperature, as for 300-mers, with  $W_B^* = 1.0$ . We also note a smaller overall difference between thin and thick phases, for shorter polymers, throughout the demixing regime.

## 4. Conclusions

This work thus demonstrates that first-order prewetting surface transitions can occur even in situations where the adjacent

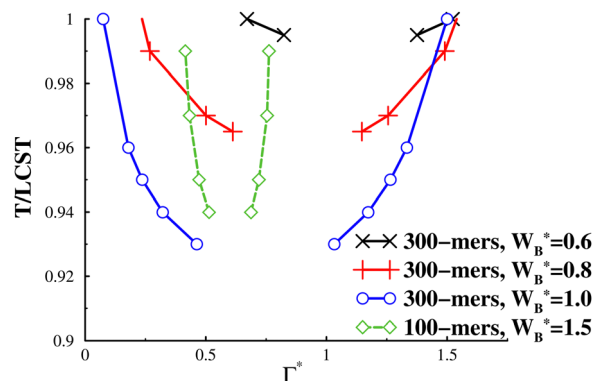


Fig. 7 Thin-thick coexistence curves, 300-mer polymer solutions, as well as a 100-mer polymer solution, below their respective bulk LCST. The notation for the 300-mer cases is the same as in Fig. 3, whereas 100-mer coexistence, with  $W_B^* = 1.5$  is indicated by diamond symbols and dashed lines (the latter to guide the eye).

bulk fluid is outside its 2-phase region (supracritical). In this case, it has been shown to occur for mixtures that exhibit an LCST. However, our results imply that coexisting surface phases don't rely on the existence of a “corresponding” metastable bulk phase. This latter type of description is often used in conjunction with the assumption of localised thermodynamics in the inhomogeneous surface phase, which is clearly not justified when the spatial extent of the relevant fluid structures are of the same order or smaller than the range of interactions. One signature of this supracritical prewetting is that, as the bulk phase increases in concentration, there is no divergence in the net adsorption of the thick phase, as occurs in complete wetting.

In this work, we have only established supracritical prewetting for systems where the surface affinity is so strong that the prewetting line is detached from the bulk coexistence line. This fact does not exclude the possibility that prewetting below the LCST also might be found for systems where there is an upper wetting temperature, *i.e.* with a prewetting line that terminates at bulk coexistence.

Finally, it is of interest to note that all interactions in our model are isotropic. In many “real” solution mixtures, there are also anisotropic interactions and, as argued by Karlström and co-workers,<sup>4,23</sup> the difference in solvophilicity between monomers in different structural states may be a result of a shift in polarity or hydrogen-bonding ability to the solute species. These are orientation-dependent pair interactions. The intrinsic degeneracies that distinguishes the A and B may then be viewed as a coarse-grained description of such differences. Moreover, our treatment here demonstrates that there are no formal requirements of anisotropy, in order to achieve the behaviours that we have investigated.

## Data availability

All generated data, as well as all codes used to generate these data, are freely available upon reasonable request. Moreover, the code, as well as a significant part of the calculated data, can be found on GitHub: [https://github.com/janneforsman/LCST\\_thinick](https://github.com/janneforsman/LCST_thinick)



## Conflicts of interest

There are no conflicts to declare.

## Acknowledgements

J. F. acknowledges financial support by the Swedish Research Council, grant number VR2021-04041.

## References

- 1 L. A. Kleintjens and R. Koningsveld, *Coll. Polym. Sci.*, 1980, **258**, 711–718.
- 2 P. H. van Koynenburg and R. L. Scott, *Phil. Trans. R. Soc. Lond. A*, 1980, **298**, 495.
- 3 H. Nakanishi and M. E. Fisher, *Phys. Rev. Lett.*, 1982, **49**, 1565–1568.
- 4 G. Karlström, *J. Phys. Chem.*, 1985, **89**, 4962–4964.
- 5 G. Jackson, *Mol. Phys.*, 1991, **72**, 1365–1385.
- 6 K. Morishige, H. Fujii, M. Uga and D. Kinukawa, *Langmuir*, 1997, **13**, 3494–3498.
- 7 E. E. Dormidontova, *Macromolecules*, 2002, **35**, 987.
- 8 S. Saeki, N. Kuwahara, S. Konno and M. Kaneko, *Macromolecules*, 1973, **6**, 246–250.
- 9 F. Xie, C. E. Woodward and J. Forsman, *Langmuir*, 2013, **29**, 2659–2666.
- 10 F. Xie, C. E. Woodward and J. Forsman, *Soft Matter*, 2016, **12**, 658–663.
- 11 S. Haddadi, C. E. Woodward and J. Forsman, *Fluid Phase Equilib.*, 2021, **540**, 112983.
- 12 H. Wennerström, K. Thuresson, P. Linse and E. Freyssingeas, *Langmuir*, 1998, **14**, 5664.
- 13 J. E. Lane and T. H. Spurling, *Aust. J. Chem.*, 1981, **34**, 1529.
- 14 C. G. V. Burgess, D. H. Everett and S. Nutall, *Pure Appl. Chem.*, 1989, **61**, 1845–1852.
- 15 M. Kotelyanskii and S. K. Kumar, *Phys. Rev. Lett.*, 1998, **80**, 1252–1255.
- 16 J. W. Cahn, *J. Chem. Phys.*, 1977, **66**, 3667.
- 17 C. Ebner and W. F. Saam, *Phys. Rev. Lett.*, 1977, **38**, 1486–1489.
- 18 P. G. deGennes, *Rev. Mod. Phys.*, 1985, **57**, 827.
- 19 D. Beysens and D. Esteve, *Phys. Rev. Lett.*, 1985, **54**, 2123–2126.
- 20 R. Evans, U. M. B. Marconi and P. Tarazona, *J. Chem. Phys.*, 1986, **84**, 2376–2399.
- 21 A. Drzewiński, A. Maciołek, A. Barasiński and S. Dietrich, *Phys. Rev. E*, 2009, **79**, 041145.
- 22 J. Indekeu and J. van Leeuwen, *Phys. C: Superconductivity*, 1995, **251**, 290–306.
- 23 M. Andersson and G. Karlstrom, *J. Phys. Chem.*, 1985, **89**, 4957–4962.

